Nanoscale

PAPER

View Article Online
View Journal | View Issue

Cite this: *Nanoscale*, 2026, **18**, 3169

N-doped carbon dots for deep-blue emission and CD-LED device with 402 nm electroluminescence

Savita Chand, Kishan Lal Kumawat, Smarak Islam Chaudhury, Bhaskar Chelleng, Kaviya Rajendran, Upasana Deori and Pachaiyappan Rajamalli *

Among the three primary colors, achieving the blue emissive organic light-emitting diodes is necessary as well as challenging. Deep-blue light-emitting diodes (emission wavelength < 450 nm) are crucial for display and AR/VR applications. However, several factors limit the functionality of blue OLED devices. The higher photon energy coming from the recombination of holes and electrons degrades the organic emitters in blue OLEDs; to overcome this issue, researchers are moving towards low-dimensional nanomaterial-based devices. Among these materials, carbon dots are easy to synthesize, economical, and non-toxic; making them suitable as cost-effective and environment friendly materials for displays. Herein, we synthesize an easy-to-prepare nitrogen-doped carbon dot using the solvothermal method. 2-Amino-5-bromopyrazine is taken as a nitrogen dopant along with terephthalic acid in DMF to obtain deep-blue emissive carbon dots with a PLQY of 60%. Structural characterizations confirm the spherical shape of the carbon dots, and the electroluminescence measurements reveal the deep blue emission maxima around 402 nm. Furthermore, the CD-LED device shows a maximum luminance of 824 cd m^{-2}, a maximum current density of 534 mA cm^{-2} and an external quantum efficiency of 2.58%, with Commission Internationale de l'Éclairage (CIE) coordinates of (0.15, 0.08). All these device parameters are better than most of the previously reported values. Hence, solution-processed pyrazine-based nitrogen-doped CDs prove to be an ideal candidate for low-cost and efficient blue LEDs.

Received 28th November 2025,
Accepted 27th December 2025

DOI: 10.1039/d5nr05028f

rsc.li/nanoscale

1. Introduction

Deep-blue emitters with high efficiency are being extensively applied in a wide range of applications, for instance, high-quality display purposes, ultrafast information storage, visible-light communication, solid-state lighting, pharmaceutical applications, printing, and analytical chemistry.[1,2] Being one of the three primary colours, obtaining blue emissive materials is highly required,[3,4] but in reality, blue emissive materials face significant limitations due to their high-energy photons. Organic materials experience degradation or configurational changes due to the high-energy photons emitted from the blue emission upon the recombination of holes and electrons. Moreover, the synthesis of organic materials is tedious, requiring multistep reaction synthesis, expensive catalysts or precursors, and considerable time. In this scenario, zero-dimensional deep-blue emitting quantum dots and carbon dots prove to be efficient and a better choice owing to their high photoluminescence quantum yield (PLQY), easy synthesis, narrow PL emission, higher stability, and facile solution-processed device fabrication.[5–9] However, quantum dots generally contain toxic heavy metals,[10–13] raising concerns towards environmental safety; thus, non-toxic carbon dots are considered a better choice for a deep-blue OLED device.

Carbon dots are zero-dimensional materials that show a quantum confinement effect due to their small size of less than 10 nm.[14–17] Carbon dots are made of graphene sheets with various functional groups such as epoxy, carboxylic, amide, hydroxy, carbonyl, and others. Depending on the functional groups, the properties of carbon dots can be tuned. Various research groups have demonstrated that doping CDs with a heteroatom creates defects at the surface of CDs. By changing the surface functionalization and conditions, their size and shape can be tuned, along with their photoluminescence spectra, which can range from UV-visible to NIR.[14–17] Surface defects originating from the sp^2- and sp^3-hybridized carbon core introduce localized trap states between bandgap energy levels, which serve as exciton capture centres through nonradiative recombination. As a result, these defects can decrease the photoluminescence quantum yield of carbon dots.[18–21] Doping heteroatoms such as nitrogen, phosphorus, and sulphur creates additional localized trap states and

Materials Research Centre, Indian Institute of Science, Bangalore, 560012, India.
E-mail: rajamalli@iisc.ac.in

increases electron density, which prevents excitons from undergoing non-radiative recombination, leading to a higher probability of radiative recombination and enhanced photoluminescence quantum yield (PLQY).[14–17,20,21] Surface functionalization by amine derivatives is a strategy used to modify the electron-withdrawing oxygen-bearing functional groups on the surface of carbon dots by introducing electron-donating amino groups.[22–25] This modification increases the extent of radiative recombination by enhancing electron density, thereby increasing the quantum yield of the carbon dots.[19,20,22–26] When the size of the carbon dot is smaller than the exciton Bohr radius, the quantum confinement effect of sp^2-hybridized carbon core restricts the delocalization of π-electrons and produces more localized electrons. This results in an alteration of the exciton energy level and leads to size-tunable photoluminescence emission.[24–26]

After the discovery of carbon dots in 2006, by Xie and co-workers,[27] widespread attention was given to exploring the properties and various applications of this new nanomaterial. High chemical stability and photostability, along with tunable emission, made it a suitable choice for optoelectronic devices.[28,29] In 2011, Liu, Ma and their group reported[30] the first-ever carbon dot-based white CD-LED.[30] Although the device parameters were not hugely impressive (maximum external quantum efficiency/EQE_{max} = 0.083% and current density = 5 mA cm^{-2}), it laid the foundation for carbon dot-based LEDs. Further, in 2013, Yu, Rogach, and their group reported a CD-LED which can switch colour depending on its input voltage.[31] This CD-LED showed blue emission, achieving a maximum current density of 150 mA cm^{-2}. Similarly, in 2016, Yuan *et al.* fabricated a colour-tunable CD-LED from blue to red LED.[32] However, fabricating a blue LED with deep-blue emission is most desired as well as challenging. In 2017, Ding *et al.* synthesized CDs consisting of phthalic acid and ethylenediamine; thereafter fabricated a CD-LED. The CD-LED emits light in the range of 6–9 V, showing the EL maxima around 420 nm.[33] In 2018, using phloroglucinol-derived carbon dots, Yang *et al.* synthesized a blue CD-LED and obtained EL maxima at 472 nm.[34] In 2020, Sargent *et al.* reported a deep-blue CD-LED with EL maxima of 433 nm and achieved an EQE of 4% using citric acid and diaminonaphthalene as precursors.[35] In 2021, Kang *et al.* reported a blue CD-LED and achieved blue CD LED with EL maxima at 456 nm with 0.86% EQE using malonylurea, citric acid, ethylenediamine as the precursors.[36] In the same year, the same group reported a blue CD-LED with EL maxima of 452 nm and an EQE of 2.1% using perylene-3,4,9,10-tetracarboxylic dianhydride, and 2,3-diaminophenazine as precursors.[37] In 2023, Tong *et al.* reported deep-blue carbon dots (CDs) with EL centered at 436 nm and an EQE of 1.76% using D,L-malic acid, and *o*-phenylenediamine as the precursors.[38] In the same year, Lu *et al.* reported a blue CD-LED and achieved an EQE_{max} of 2% with EL maxima at 453 nm using perylene and 1,3-diaminopropane as the precursors.[39] However, the earlier reports have some limitations; either they lack in achieving satisfactory CIE values (x, y) of $y < 0.1$ or their emission maxima lie far from the blue end (400 nm). For the deep-blue emission, a CIE (x, y) value of $y < 0.10$ is desirable. Therefore, designing cost-effective and eco-friendly emissive materials with CIE coordinates of $y < 0.10$ and EL maxima close to 400 nm remains a primary goal in the development of next-generation deep-blue LEDs.[40]

Here, in this paper, we present a feasible approach to synthesize non-toxic and eco-friendly nitrogen-doped deep-blue emissive carbon dots and achieve a CD-LED with deep-blue emission of 402 nm. The CDs are synthesized by the solvothermal method using terephthalic acid ($C_8H_6O_4$) and 2-amino-5-bromopyrazine ($C_4N_2H_4$) as precursors. 2-Amino-5-bromopyrazine is introduced to achieve heteroatom doping (nitrogen), which enhances the photoluminescence quantum yield of CDs. The CDs show a high PLQY of 60%. Thereafter, we fabricate a blue CD-LED having the device architecture of ITO/PEDOT:PSS (40 nm)/PVK (30 nm)/CDs:CBP/TPBi (50 nm)/Liq (2 nm)/Al (100 nm) which shows excellent device parameters with a remarkable EQE_{max} of 2.58%, a maximum luminance of 824 cd m^{-2}, a maximum current density of 534 mA cm^{-2}, and EL maxima centered at 402 nm in the deep-blue region with CIE values of (0.15, 0.08).

2. Experimental

2.1 Materials

Terephthalic acid (1,4-benzenedicarboxylic acid) and 2-amino-5-bromopyrazine were purchased from S. D. Fine-Chem Limited and BLD Pharmaceuticals, respectively. *N*,*N*, Dimethylformamide (DMF) was procured from Hyma Synthesis Private Limited. UV spectroscopy-grade toluene was purchased from Spectrochem. Ethyl acetate (EA), dimethyl chloride (DCM), and methanol (MeOH) were obtained from PureChem. Poly(*N*-vinylcarbazole) (PVK, M.W. 110 000) was purchased from Sigma-Aldrich. 1,3,5-Tris(1-phenyl-1*H*-benzimidazol-2-yl)benzene (TPBi) and lithium quinolate (Liq) were purchased from BLD Pharmaceuticals. Poly(3,4-ethylenedioxythiophene):polystyrene sulfonate (PEDOT:PSS, Al 4083) was purchased from Ossila. Aluminum pellets were procured from Kurt J. Leskar. The etched ITO glass substrate was purchased from Zhuhai Kaivo Optoelectronic Technology Co., Ltd. TPBi and Liq were sublimed using a vacuum sublimation set-up before use, and other materials were used without further purification.

2.2 Synthesis of carbon dots

Blue emissive nitrogen-doped CDs were synthesized by the solvothermal method using terephthalic acid and 2-amino-5-bromopyrazine as the precursors. A total of 166 mg (1 mmol) terephthalic acid and 348 mg (2 mmol) 2-amino-5-bromopyrazine were dissolved in a solution containing *N*,*N*-dimethylformamide (40 ml) and DI water (40 ml). The mixture solution was then transferred into a 100 ml stainless-steel autoclave and heated at 185 °C for 16 hours. The crude product was washed with ethyl acetate and water using a separating funnel,

followed by filtration using Whatman filter paper. The resulting clear solution was obtained and then evaporated to get a concentrated CD solution. The blue emissive CDs were further purified using silica gel column chromatography with DCM : MeOH solvent mixture. The final product was dispersed in toluene.

2.3 Device fabrication

A patterned ITO glass substrate of a specific dimension was taken (size = 15 × 20 mm, sheet resistance = 15 Ω cm^{-2}, and active area = 3.0 × 1.5 mm^2 with an individual pixel area of 4.5 mm^2). At first, to remove any dust particles and organic residues, patterned ITO substrates were cleaned by an ultrasonic bath using Hellmanex III soap solution, isopropyl alcohol, and acetone, respectively. For surface activation, the substrates were kept under UV-ozone treatment for 20 minutes. After ozone cleaning, a 40 nm PEDOT:PSS layer was spin-coated on cleaned ITO substrates at 4000 rpm for 1 min and annealed at 140 °C for 20 min. Similarly, a 30 nm PVK (5 mg ml^{-1} in chlorobenzene) layer was spin-coated on top of PEDOT:PSS at 4000 rpm for 1 min and annealed at 140 °C for 20 min. The blue emissive carbon dot layer was doped with CBP host material (20 weight% of CDs in CBP) and spin-coated at 3000 rpm for 1 min (30 nm). To preserve the bottom layer while spin-coating the emissive layer, an orthogonal solvent strategy was employed, in which the differential solubility of the materials was exploited to protect the bottom layer from dissolution.[41] Here, the PVK layer is soluble in chlorobenzene, but exhibits partial solubility in toluene, whereas toluene effectively dissolves the emissive layer while maintaining the PVK layer insoluble and intact. Therefore, the PVK hole transport layer was spin-coated in chlorobenzene solution, while the CBP:carbon dot emissive layer was spin-coated using toluene as the solvent. Moreover, the PVK layer was thermally annealed for 15 minutes at 140 °C. The heat treatment makes the PVK layer resistant to subsequent solvent exposure through the cross-linking of the polymer. The substrates were then loaded into a thermal evaporation chamber to deposit the TPBi (50 nm), Liq (2 nm), and Al (100 nm) cathode. The layers were deposited at a vacuum of 5 × 10^{-6} torr. The deposition rate of TPBi, Liq, and Al was constantly monitored and kept at 1.5, 0.1, and 2–5 Å s^{-1}, respectively.

2.4 Characterization

The morphology of the carbon dots was determined using transmission electron microscopy (TEM; JEOL JEM-2100F) at an accelerating voltage of 200 kV. X-ray diffraction of the as-synthesized carbon dots was obtained using the X'Pert PRO PANanalytical instrument with a Cu Kα source (wavelength = 1.541 Å). The synthesized CDs were drop-cast on a sapphire substrate and dried to make a thin film. The XRD patterns were analysed to determine the crystal structure of the synthesized CD sample. UV-visible absorbance spectra were measured using a JASCO V-730 spectrophotometer, and the photoluminescence spectra were obtained using a Hitachi F-7100 fluorescence spectrophotometer. FTIR measurements were done using a Thermo Scientific Nicolet iS50 FTIR spectrometer. The lifetime measurements were obtained using an Edinburgh FS5 spectrofluorometer in TCSPC mode with an EPL375 laser as the excitation source. Photoluminescence quantum yield was measured using a Horiba FluoroMax Plus spectrofluorometer. The cyclic voltammetry measurement was carried out in deoxygenated dichloromethane (DCM) with 0.1 M tetrabutylammonium hexafluorophosphate (TBAP) as the supporting electrolyte in a three-electrode system using a BioLogic SP-50 potentiostat. Glassy carbon, platinum wire (Pt), and Ag/AgCl/KCl (saturated) were used as working, counter, and reference electrodes, respectively. Ferrocene was taken as the internal standard. The scan rate of 50 mV s^{-1} was kept for all the measurements. The XPS analysis of the samples was done using K-Alpha spectrometer (Thermo Fisher Scientific) with Al Kα as an X-ray source (1486.6 eV). The synthesized carbon dots were drop-cast on a silicon substrate for the XPS measurements.

2.5 LED device characterization

A silicon photodiode was used in conjunction with a Keithley 2450 source meter and a Keithley 2100 multimeter to measure the current–voltage–luminance (*I–V–L*) and external quantum efficiency–luminance (EQE–*L*) characteristics. The electroluminescence (EL) spectra were obtained using a Hitachi F-7100 fluorescence spectrophotometer.

3. Results and discussion

The schematic of the synthesis of nitrogen-doped, blue-emissive carbon dots using the solvothermal method is shown in Fig. 1(a). Terephthalic acid and 2-amino-5-bromopyrazine are used as the precursors in a 1 : 1 ratio of DMF : DI water mixture. 2-Amino-5-bromopyrazine acts as a nitrogen dopant, and terephthalic acid acts as a carbon source. After the reaction, the synthesized carbon dots were purified using silica column chromatography and dispersed in toluene, which were used for further characterization. The proposed reaction scheme for the formation of nitrogen-doped carbon dots is shown in Fig. 1(b).

The morphology of the synthesized nitrogen-doped CDs was analysed using transmission electron microscopy (TEM), as shown in Fig. 2(a) and (b). The TEM micrograph reveals a uniform, spherical particle morphology with well-defined boundaries and minimal surface aggregation. The average size of the particles is calculated to be 2.4 ± 0.56 nm from 200 distinguishable particles. The standard deviation was found to be 0.56 nm for the synthesized carbon dots. The reason for the small deviation error is due to the very small particle size of the CDs.[42] Fig. 2(c) shows the X-ray diffraction (XRD) pattern of nitrogen-doped CDs, where the peaks at 2θ = 11.00° and 18.02° were observed. The peak at 11.00° corresponds to the (002) plane of graphene oxide and confirms the formation of graphene oxide and the presence of oxide functional groups, such as epoxy, hydroxy (–OH), and carboxylic (–COOH).[43,44]

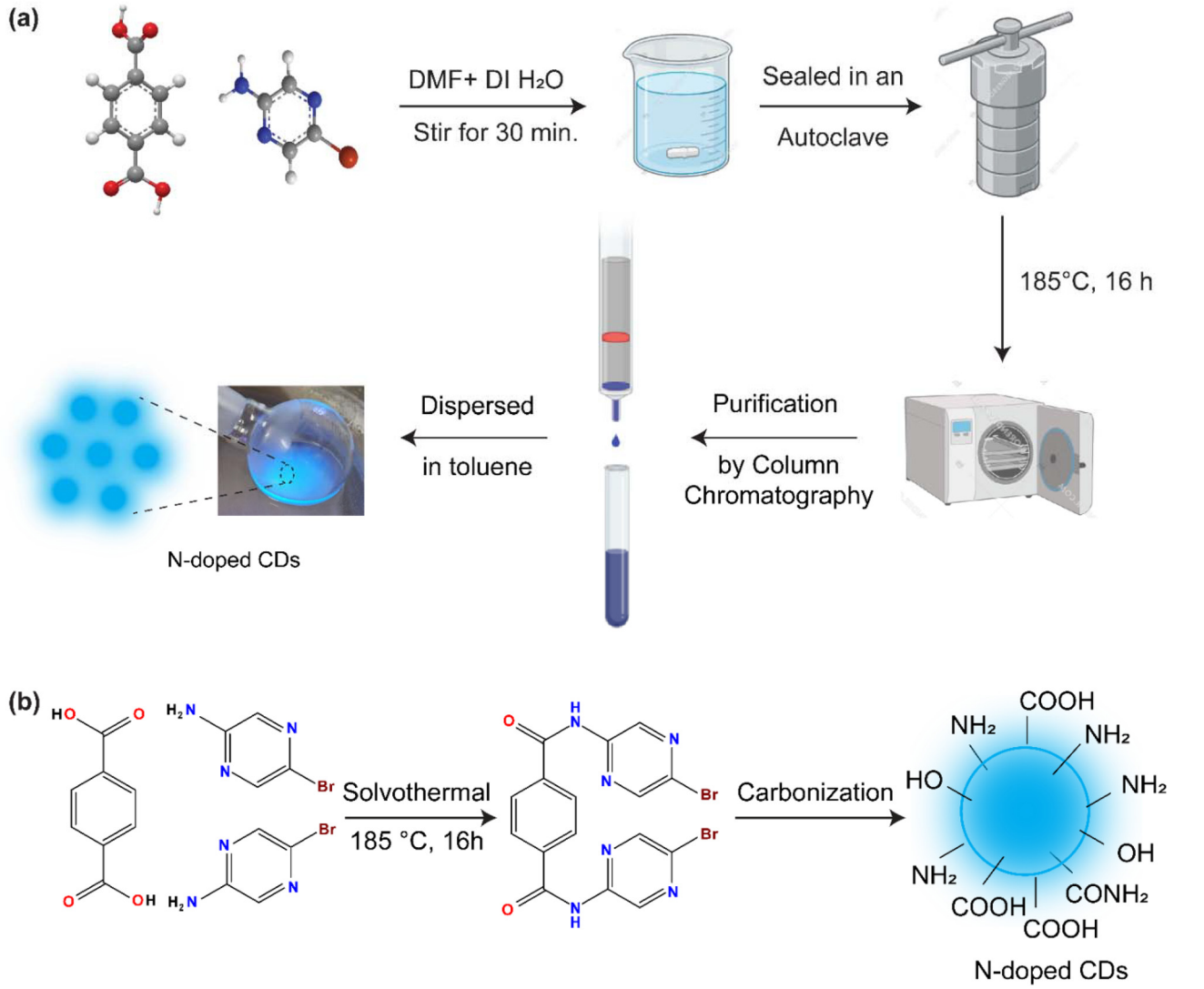

Fig. 1 (a) Schematic of the synthesis of the nitrogen-doped blue-emissive CDs by the solvothermal method. (b) Proposed reaction scheme for the formation of nitrogen-doped blue-emissive CDs.

The *d*-spacing was calculated using Bragg's law ($n\lambda = 2d \sin\theta$), where $n = 1$, $\lambda = 1.541$ Å (Cu Kα radiation), and $\theta = 2\theta/2$ is the Bragg angle.[45] The calculated *d*-spacing for $2\theta = 11.0°$ was found to be $d = 8.05$ Å. The results indicated that the interlayer spacing was extended due to the intercalation of the oxygen-containing functional groups into the layers.[43,44] The peak at 18.02°, with a *d*-spacing of 4.9 Å, corresponds to partially intercalated graphitic carbon layers.[46] Furthermore, to determine the functional groups present on the surface of nitrogen-doped CDs, Fourier transform infrared spectroscopy (FTIR) analysis was performed (Fig. 2(d)). The FTIR spectrum exhibits a broad peak centered around 3300–3470 cm^{-1}, attributed to the symmetric and asymmetric stretching of O–H and N–H groups (a zoomed view is shown in the inset).[42] The broadening of the peak indicates the existence of hydrogen bonding between various oxygen- and nitrogen-containing functional groups. The peak around 2998 cm^{-1} is due to C–H stretching. The strong peaks observed at 1743, 1377, 1238, and 1048 cm^{-1} are attributed to C═O, C–N, C–O, and C–O–C stretching vibrations, respectively.[36,42] These peaks indicate the presence of the carboxyl and amide groups. Furthermore, the peaks at 1450, 950, 937, and 609 cm^{-1} are due to C–H bending vibrations.[36,42,47,48] The presence of C–N stretching confirms the heteroatom doping with nitrogen in the synthesized CDs. This confirms the presence of –COOH (carboxyl), –OH (hydroxyl), $-CONH_2$ (amide), and NH_2 (amine) groups on the surface of the synthesized carbon dots.

Fig. 3(a) depicts the UV-visible absorbance and photoluminescence spectra of CDs in toluene. CDs exhibit maximum absorbance at around 286 nm, which is due to the $\pi \rightarrow \pi^*$ transition in the aromatic rings of CDs, and at 368 nm due to the $n \rightarrow \pi^*$ transition from the C═O and C–N functional groups on the surface.[36,42,49] The fluorescence spectra exhibit emission at 415 nm, with a Stokes shift energy of 0.38

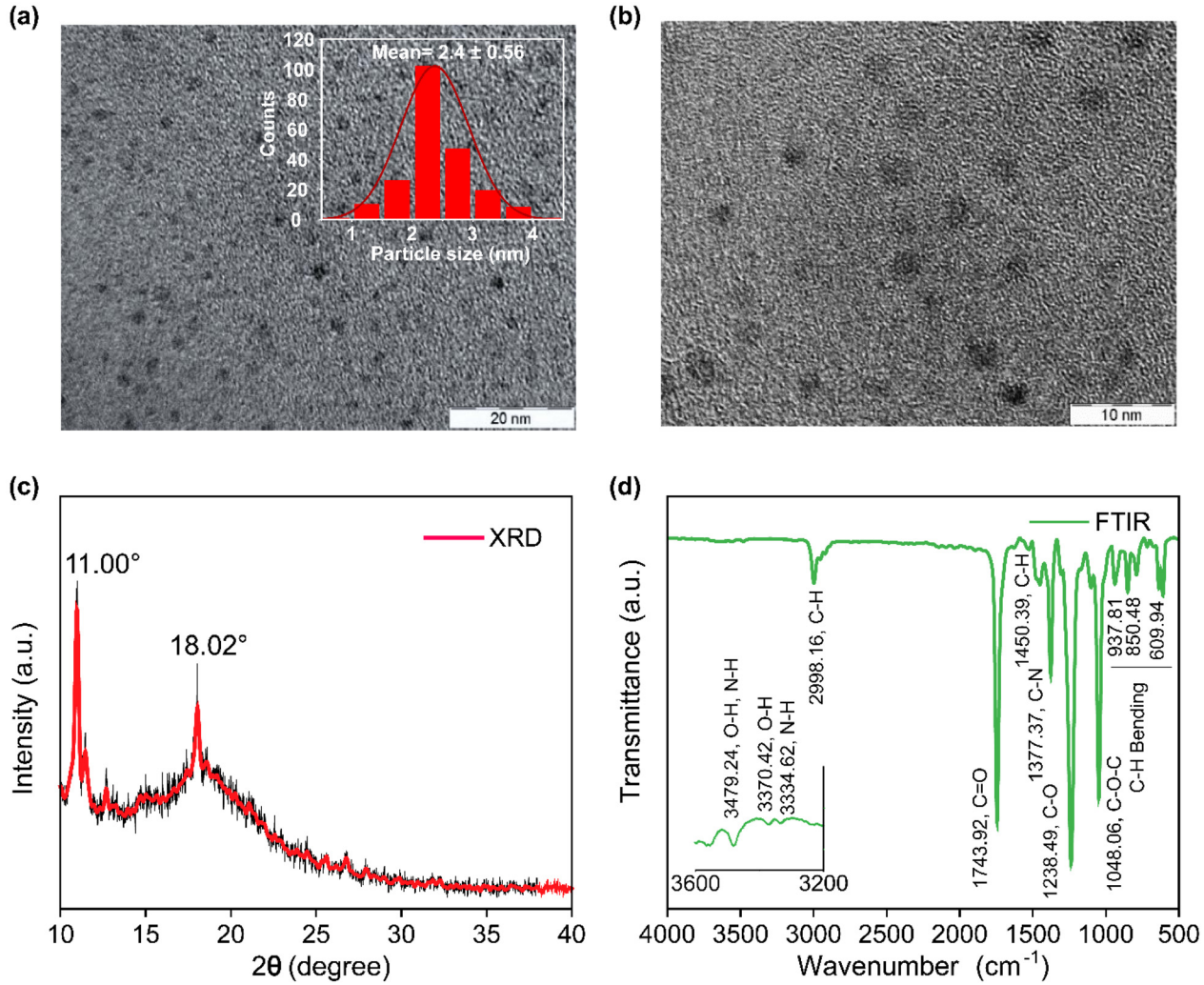

Fig. 2 TEM characterization of carbon dots. (a) TEM image showing dispersed carbon dots with uniform size distribution at a scale bar of 20 nm (inset: particle size distribution histogram measured from n = 200 distinguishable particles). The average diameter is 2.0 ± 0.38 nm. (b) TEM image at a scale bar of 10 nm. (c) X-ray diffraction (XRD) pattern. (d) Fourier transform infrared (FTIR) spectra of N-doped CDs.

eV. This relatively large Stokes shift suggests that emission occurs through surface-state-mediated relaxation pathways rather than direct band-edge recombination, consistent with exciton localization at surface functional groups or defect sites.[49–51] The full width at half maximum (FWHM) of the nitrogen-doped blue CDs was found to be 73 nm. The average lifetime of fluorescence is determined using time-correlated single-photon counting (TCSPC) by a 375 nm laser as the excitation source. Fig. 3(b) depicts the fluorescence decay curve of the N-doped CDs. The counts were fitted using a bi-exponential function $F(y)$ as represented by eqn (1):

$$F(y) = A + B_1 e^{-x/\tau_1} + B_2 e^{-x/\tau_2} \quad (1)$$

where τ_1 and τ_2 values are calculated as 1.78 and 7.92 ns, respectively. The relative % of B_1, and B_2 are 2.51 and 97.49, respectively. The average fluorescence decay lifetime of CDs is calculated as 7.29 ns. This shorter lifetime in the nanosecond range confirms the fluorescent emission mechanism of the nitrogen-doped CDs. Furthermore, the photoluminescence quantum yield (PLQY) of the carbon dots was measured in toluene solvent and found to be 60% (see Fig. S1, SI). The high PLQY of CDs corroborates that this CD can be used for high-efficiency blue LEDs. Cyclic voltammetry measurements (Fig. 3(c)) were performed to determine the HOMO and LUMO energy levels of nitrogen-doped carbon dots, using ferrocene as an internal standard. From the onset voltage (E_{ox}) of the cyclic voltammogram, the HOMO energy level was obtained as follows:

$$E_{HOMO} = -[(E^{onset}_{oxidation} - E^{Ferrocene}_{1/2}) + 4.8]\ \text{eV} \quad (2)$$

The CV curve of nitrogen-doped CDs gives the value of oxidation onset, $E^{onset}_{oxidation}$ at +1.199 V *vs.* Ag/AgCl. After calibration against the ferrocene/ferrocenium (Fc/Fc^+), the value of $E^{Ferrocene}_{1/2}$ was found to be 0.49 V (Fig. S2, SI). By substituting these values into eqn (2), the HOMO energy level was calculated to be −5.51 eV (relative to the vacuum level). The optical

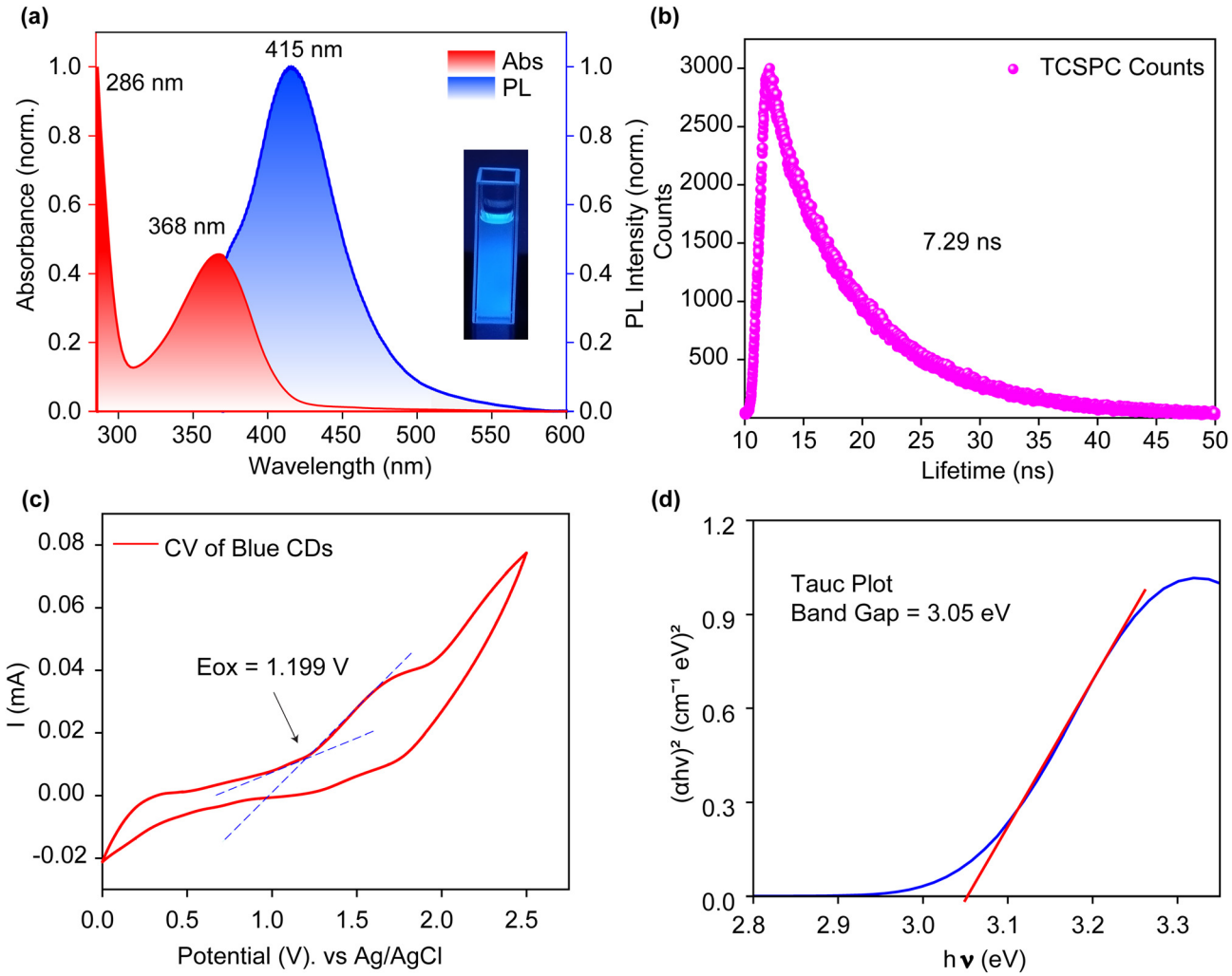

Fig. 3 (a) Absorption and fluorescence spectra of the N-doped blue CDs. (b) Transient PL decay curve. (c) Cyclic voltammetric (CV) analysis of the nitrogen-doped CD in tetrabutylammonium hexafluorophosphate (TBAP), 0.1 mol L^{-1} in CH_2Cl_2 using glassy carbon, platinum wire (Pt), and Ag/AgCl/KCl (saturated) as working, counter, and reference electrodes, respectively. (d) Tauc plot of the nitrogen-doped CDs.

band gap of the CDs is determined using the Tauc plot of the UV-Vis absorption data (Fig. 3(d)), where the light quantum energy ($h\nu$) and $(\alpha h\nu)^{1/2}$ are plotted on the x- and y-axes, respectively (α is the absorbance in the UV-Vis spectra).[36] The value of the bandgap, calculated from the tangent of the Tauc plot, was found to be 3.05 eV. This yields an estimated LUMO energy level of −2.46 eV (calculated from $E_{LUMO} = E_{HOMO} - E_g$). These HOMO and LUMO values are desirable for the smooth injection of charge carriers in the device.

The elemental composition of CDs was determined by X-ray photoelectron spectroscopy (XPS), as shown in Fig. 4(a)–(d). The XPS survey spectrum (Fig. 4(a)) exhibits three major peaks at 285.08, 400.08, and 532.1 eV, corresponding to the C 1s, N 1s, and O 1s core levels, respectively. The high-resolution XPS (HR-XPS) of C 1s in Fig. 4(b) demonstrates three peaks positioned at 284.36, 285.11, and 288.31 eV, which are attributed to the functional groups of C–C/C=C, C–O/C–N, and C=O, respectively. Fig. 4(c) shows the HR-XPS of O 1s, the peaks at 531.71 and 533.23 eV confirm the presence of C–O and C=O bonds. Furthermore, the doping of N into the CDs is revealed by the N 1s HR-XPS spectra in Fig. 4(d). The single peak at 399.84 eV reveals the presence of the C–N (pyridine or pyrrolic) bond in the CDs.[42,47,48] Fig. S3 (SI) shows the fitted survey spectra, and the percentage composition of C, O, and N is determined as 80.89 : 12.55 : 6.56 (Table S1, SI). Hence, this confirms the presence of N as a dopant in the synthesized CDs.

The synthesized blue-emissive carbon dots were then utilized as an emissive layer in the multi-layered CD-LED device using a solution-processing fabrication technique.[52] The device architecture was as follows: ITO (indium tin oxide)/PEDOT:PSS (poly(3,4-ethylenedioxythiophene)polystyrene sulfonate) (40 nm)/PVK (poly(*N*-vinylcarbazole)) (30 nm)/blue CDs doped with CBP (4,4′-bis(*N*-carbazolyl)-1,1′-biphenyl)/TPBi (1,3,5-tris(1-phenyl-1*H*-benzimidazol-2-yl)benzene) (50 nm)/Liq (lithium 8-quinolinolate) (2 nm)/Al (100 nm). The ITO acts as the anode, above which different layers are deposited for the fabrication of the device. The PEDOT:PSS and PVK act as hole-

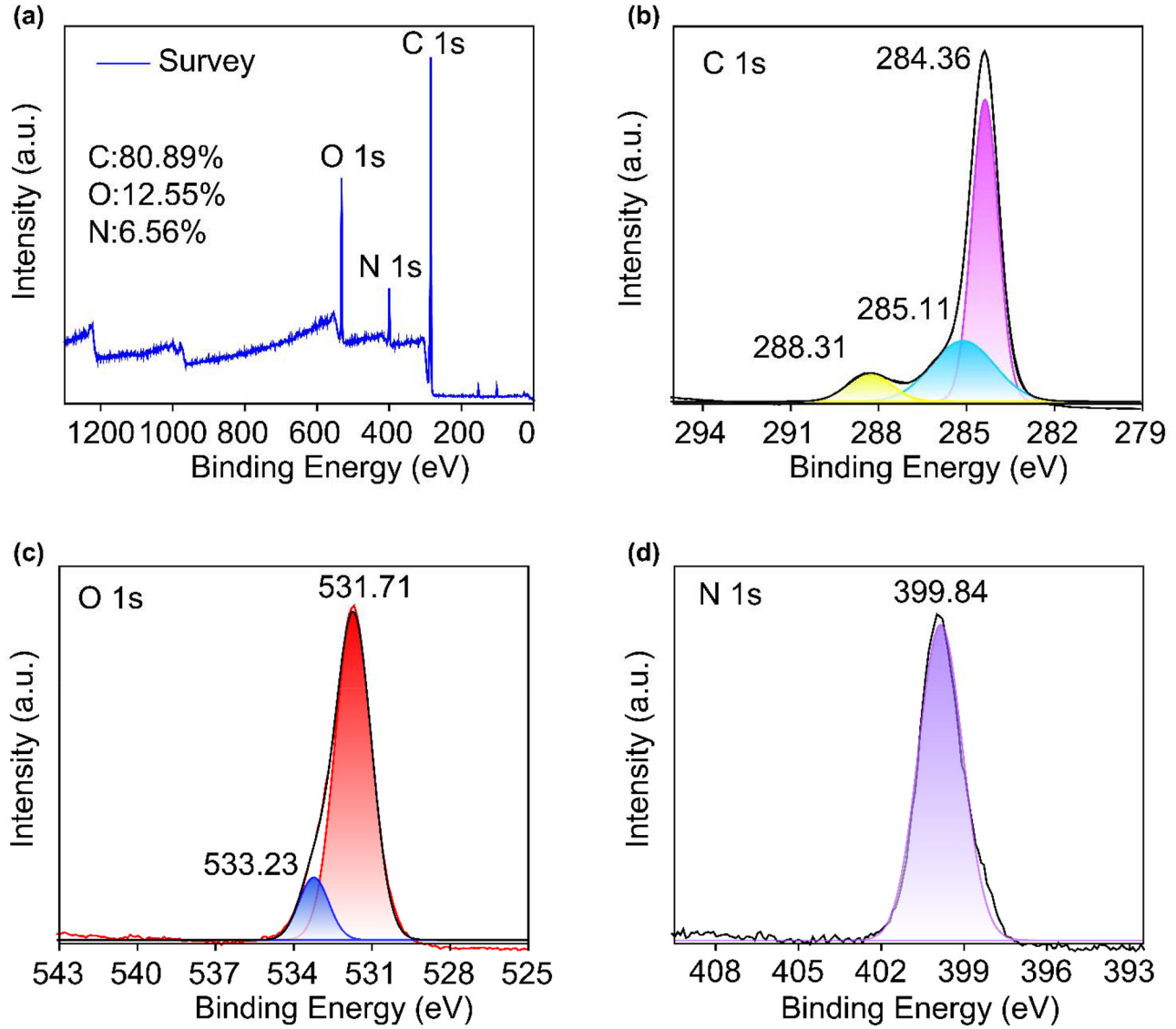

Fig. 4 X-ray photoelectron spectra (XPS) of the nitrogen-doped CDs. (a) Survey scan. (b) High-resolution XPS of C 1s. (c) High-resolution XPS of O 1s. (d) High-resolution XPS of N 1s core energy level.

injection layers (HILs) and hole-transport layers (HTLs), respectively. TPBi and Liq act as electron transport layer (ETL) and electron injection layer (EIL), respectively. The aluminium metal is used for the device contact and works as the cathode. The CBP host material is used for the carbon dot emissive layer to suppress aggregation-caused quenching (ACQ) through physical isolation of individual carbon dots. The reason for selecting CBP as a host is its bipolar charge transport characteristics, which help balance electron and hole injection, thereby reducing exciton quenching and improving device efficiency.[53,54] The PL spectra of the CD film doped with the CBP host matrix are shown in Fig. S4 (SI). The electroluminescence properties of the fabricated CD-LED are shown in Fig. 5. The energy level diagram (along with the HOMO–LUMO values) of each layer is shown in Fig. 5(a), where the HOMO and LUMO levels of all layers are aligned with a minimum energy barrier, indicating the smooth injection of holes and electrons into the emissive layer. The molecular structures of all the layers used for device fabrication are shown in Fig. 5(b). Fig. 5(c) shows the external quantum efficiency (EQE) *vs.* luminance (L) curve (the inset shows the image of the fabricated blue CD-LED), revealing an EQE of 2.58% for the fabricated blue CD-LED. The current density–voltage–luminance (J–V–L) characteristics of the device for CDs are shown in Fig. 5(d). A current density of 534 mA cm^{-2} was obtained, and the turn-on voltage, at which the device exhibits brightness greater than 1 cd m^{-2}, is found to be 8 V. The fabricated CD-LED achieved a maximum luminance of 824 cd m^{-2}. Fig. 5(e) shows the electroluminescence (EL) spectra of the device at 10 V, and the emission maxima were located at 402 nm. The FWHM of the nitrogen-doped CD-LED was found to be 68 nm in the EL spectra. The EL spectra were also recorded at various voltages,

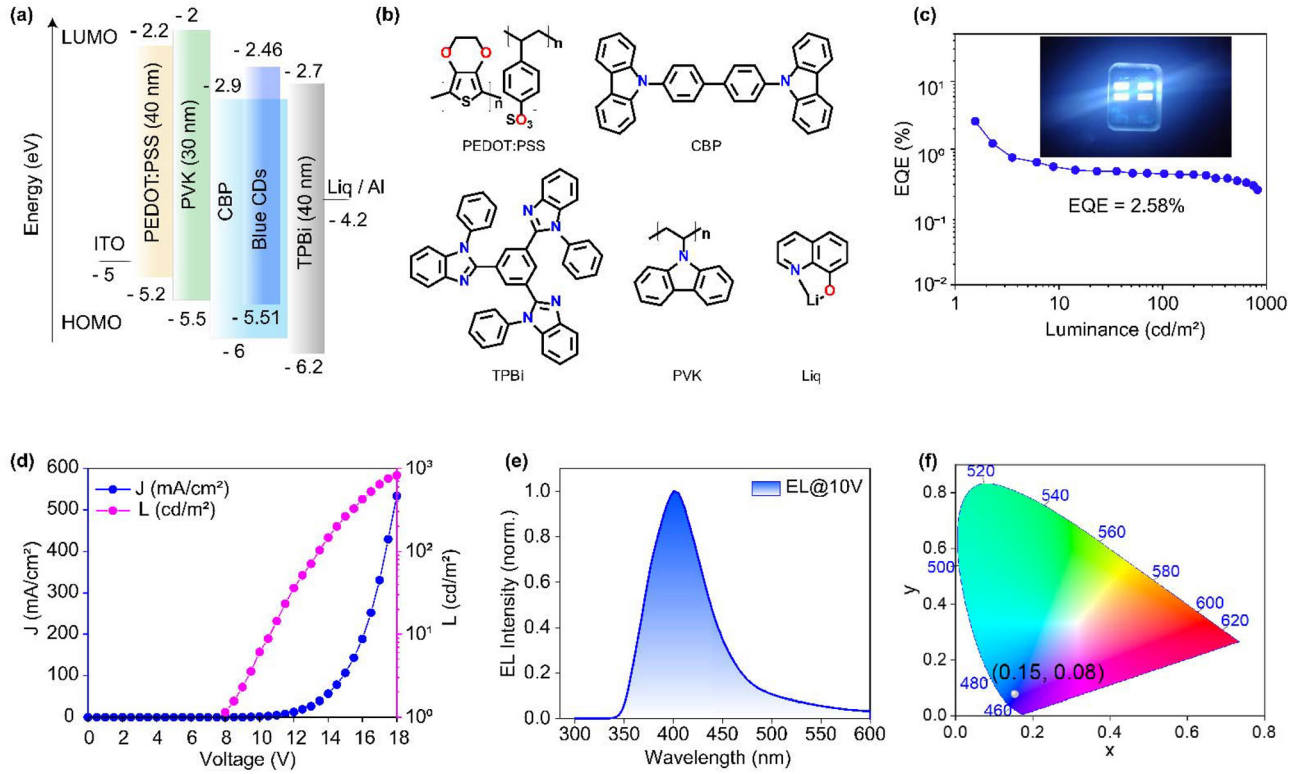

Fig. 5 (a) Energy-level diagram for the device architecture of the CD-LED. (b) Molecular structures of the layers. LED characterizations for the CD-LED. (c) EQE *versus* luminance curve (inset showing fabricated blue LED device). (d) Variation of luminance and current density with applied voltage. (e) Electroluminescence spectra of the device. (f) Commission Internationale de l'Éclairage (CIE) diagram of the fabricated CD-LED.

ranging from 8 V to 12 V (Fig. S5, SI), and no shift was observed in the EL peak of the CD-LED, indicating that the device remains stable across different operating voltages. The Commission Internationale de l'Éclairage (CIE) coordinates of the fabricated CD-LED are determined by a chromaticity plot, as shown in Fig. 5(f), and are found to be (0.15, 0.08), lying in the deep-blue region.

The device parameters of the earlier reported blue CD-LED are listed below in Table 1. Synthesis methods, taken precursors, along with the emission maxima, turn-on voltage, maximum current density, maximum luminance, and maximum external quantum efficiency of the CD-LEDs are mentioned in the table. The overall comparison shows that our blue CD-LED has promising device parameters and shows

Table 1 Comparison of blue CD-LED device parameters in the literature

Synthesis method	Precursor	λ_{max} (nm)	V_{on} (V)	CD_{max} (mA cm^{-2})	L_{max} (cd m^{-2})	EQE (%)	CIE coordinates	Ref.
Refluxing at high temperature	Anhydrous citric acid, 1-hexadecylamine, octadecene	426	5.0	150	24	—	(0.19, 0.15)	31
Microwave-assisted pyrolysis	Formaldehyde, potassium hydrogen phthalate, sodium azide, boric acid	432	3.6	—	3922	1.6	(0.17, 0.14)	55
Hydrothermal	Phthalic acid, ethylenediamine	410	5.5	630	4.97	—	(0.15, 0.05)	33
Hydrothermal	Malonylurea, citric acid, ethylene diamine	456	5.3	40	223	0.86	(0.21, 0.23)	36
Hydrothermal	Perylene-3,4,9,10-tetracarboxylic dianhydride, 2,3-diamino phenazine	452	6.7	40	648	2.11	(0.14, 0.10)	37
Solvothermal	Citric acid, 2,3-diaminonaphthalene	455	4.7	—	136	—	(0.19, 0.20)	32
Solvothermal	Citric acid, diaminonaphthalene	433	4.8	100	5 240	4.04	(0.15, 0.05)	35
Solvothermal	Phloroglucinol	472	4.3	—	1882	—	—	34
Solvothermal	Citric acid, urea	440	—	—	—	—	—	56
Solvothermal	Ammonium citrate, EDTA	472, 469	—	—	—	—	—	57
Solvothermal	D,L-Malic acid, *o*-phenylenediamine	436	3	1000	1155	1.74	(0.16, 0.08)	38
Solvothermal	Perylene, 1,3-diaminopropane, sulfuric acid	453	—	80	500	2.04	(0.15, 0.13)	39
Solvothermal	3,4,9,10-Perylenetetracarboxylic diimide, 4,4′, 4″,4‴-(pyrene-1,3,6,8-tetrayl)tetrabenzoic acid	450	5.2	140	100	10.8	(0.15, 0.07)	58
Solvothermal	Terephthalic acid, 2-amino-5-bromopyrazine	402	8	534	824	2.58	(0.15, 0.08)	This work

the most blue-shifted emission so far in any carbon dot-based LED device.

4. Conclusion

In summary, the blue-emissive carbon dots were synthesized by the solvothermal method, in which 2-amino-5-bromopyrazine acts as the nitrogen dopant, while terephthalic acid acts as the carbon source. The nitrogen-doped carbon dots exhibited a high PLQY of 60% in a toluene solution, which was further utilized as an emissive layer to fabricate a CD-LED with deep-blue emission. The fabricated device exhibited a high EQE value of 2.58%, which is higher than most of the earlier reported blue CD-LEDs, and an EL maximum of 402 nm, with a CIE value of (0.15, 0.08) in the deep-blue region, representing the most blue-shifted emission obtained from any CD-LED yet. This shows that the synthesized CDs can function effectively in the electroluminescent LEDs. This research work opens up new pathways towards deep-blue emissive carbon dots for cost-efficient and eco-friendly CD-based blue LEDs through nitrogen doping.

Author contributions

Savita Chand: conceptualization, data curation, formal analysis, investigation, methodology, visualization, and writing; Kishan Lal Kumawat: conceptualization, data curation, formal analysis and writing; Smarak Islam Chaudhury: investigation, methodology, and writing; Bhaskar Chelleng: data curation; Kaviya R: data curation; Upasana Deori: formal analysis; and P. Rajamalli: resources, project administration, supervision, and review & editing.

Conflicts of interest

The authors declare no conflicts of interest.

Data availability

The raw datasets supporting the findings of this study are available from the corresponding author upon reasonable request.

Supplementary information is available. PLQY Measurements, Cyclic Voltametric analysis of Ferrocene, XPS Survey scan, PL spectra of CBP-doped carbon dots in film, EL spectra of CD-LED at different operating Voltages. See DOI: https://doi.org/10.1039/d5nr05028f.

Acknowledgements

The authors are thankful to the Department of Science and Technology (DSTFIST: SR/FST/PSII009/2010) for providing the instrumental facility at MRC, IISc. The authors acknowledge the I-STEM, and the Centre of Nanoscience and Engineering (CeNSe) department for their instrument facilities. S. C. and S. I. C. thank the Ministry of Education, Government of India, for the Prime Minister's Research Fellowship (PMRF). K. L. K. acknowledges the research associate fellowship provided by the Indian Institute of Science, Bangalore. P. R. thanks IISc and the INDIA–TAIWAN Programme of Cooperation in Science and Technology (Grant No. 2024/IN-TW/07) and the Ministry of Education, India (Grant No: MoE-STARS/STARS-2/2023-0651) for financial support.

References

1 P. Han, E. Xia, A. Qin and B. Z. Tang, Adjustable and Smart AIEgens for Nondoped Blue and Deep Blue Organic Light-Emitting Diodes, *Coord. Chem. Rev.*, 2022, **473**, 214843, DOI: 10.1016/j.ccr.2022.214843.

2 X. Yang, X. Xu and G. Zhou, Recent Advances of the Emitters for High Performance Deep-Blue Organic Light-Emitting Diodes, *J. Mater. Chem. C*, 2015, **3**(5), 913–944, DOI: 10.1039/C4TC02474E.

3 Y. Xu, X. Liang, Y. Liang, X. Guo, M. Hanif, J. Zhou, X. Zhou, C. Wang, J. Yao, R. Zhao, D. Hu, X. Qiao, D. Ma and Y. Ma, Efficient Deep-Blue Fluorescent OLEDs with a High Exciton Utilization Efficiency from a Fully Twisted Phenanthroimidazole–Anthracene Emitter, *ACS Appl. Mater. Interfaces*, 2019, **11**(34), 31139–31146, DOI: 10.1021/acsami.9b10823.

4 Z. Feng, Z. Cheng, Z. Su, L. Wan, S. Ge, H. Liu, X. Ma, F. Liu and P. Lu, Realizing Efficient Deep Blue Light–Emitting Diodes and Single Component White Light–Emitting Diodes with Low Efficiency Roll–Offs from Anthracene–Based Organic Emitters, *Adv. Opt. Mater.*, 2024, **12**(14), 2302839, DOI: 10.1002/adom.202302839.

5 Q. Guo, L. Wang, L. Yang, J. Duan, H. Du, G. Ji, N. Liu, X. Zhao, C. Chen, L. Xu, L. Gao, J. Luo and J. Tang, Spectra Stable Deep-Blue Light-Emitting Diodes Based on Cryolite-like Cerium(III) Halides with Nanosecond d-f Emission, *Sci. Adv.*, 2022, **8**(50), eabq2148, DOI: 10.1126/sciadv.abq2148.

6 A. Saha, R. Yadav, D. Aldakov and P. Reiss, Gallium Sulfide Quantum Dots with Zinc Sulfide and Alumina Shells Showing Efficient Deep Blue Emission, *Angew. Chem., Int. Ed.*, 2023, **62**(45), e202311317, DOI: 10.1002/anie.202311317.

7 K. Y. Jang, S. Y. Hwang, S. Woo, E. Yoon, C. Park, S. Y. Kim, D. Kim, H. Kim, J. Park, E. H. Sargent and T. Lee, Efficient Deep–Blue Light–Emitting Diodes Through Decoupling of Colloidal Perovskite Quantum Dots, *Adv. Mater.*, 2024, **36**(39), 2404856, DOI: 10.1002/adma.202404856.

8 X. Chen, X. Lin, L. Zhou, X. Sun, R. Li, M. Chen, Y. Yang, W. Hou, L. Wu, W. Cao, X. Zhang, X. Yan and S. Chen, Blue Light-Emitting Diodes Based on Colloidal Quantum Dots with Reduced Surface-Bulk Coupling, *Nat. Commun.*, 2023, **14**(1), 284, DOI: 10.1038/s41467-023-35954-x.

9 W. Zhang, B. Li, C. Chang, F. Chen, Q. Zhang, Q. Lin, L. Wang, J. Yan, F. Wang, Y. Chong, Z. Du, F. Fan and H. Shen, Stable and Efficient Pure Blue Quantum-Dot LEDs Enabled by Inserting an Anti-Oxidation Layer, *Nat. Commun.*, 2024, **15**(1), 783, DOI: 10.1038/s41467-024-44894-z.

10 W. Shen, Y. Qiu, J. Jiang, Z. Chen, Y. He, H. Cui, L. Liu, G. Cheng, A. N. Aleshin and S. Chen, Stable Deep-Blue $FAPbBr_3$ Quantum Dots Facilitated by Amorphous Metal Halide Matrices, *Chem. Commun.*, 2023, **59**(74), 11137–11140, DOI: 10.1039/D3CC03415A.

11 B. Gidwani, V. Sahu, S. S. Shukla, R. Pandey, V. Joshi, V. K. Jain and A. Vyas, Quantum dots: Prospectives, toxicity, advances and applications, *Adv. Mater.*, 2021, **61**, 102308, DOI: 10.1016/j.jddst.2020.102308.

12 X. Chen, X. Lin, L. Zhou, X. Sun, R. Li, M. Chen, Y. Yang, W. Hou, L. Wu, W. Cao, X. Zhang, X. Yan and S. Chen, Blue Light-Emitting Diodes Based on Colloidal Quantum Dots with Reduced Surface-Bulk Coupling, *Nat. Commun.*, 2023, **14**(1), 284, DOI: 10.1038/s41467-023-35954-x.

13 W. Zhang, B. Li, C. Chang, F. Chen, Q. Zhang, Q. Lin, L. Wang, J. Yan, F. Wang, Y. Chong, Z. Du, F. Fan and H. Shen, Stable and Efficient Pure Blue Quantum-Dot LEDs Enabled by Inserting an Anti-Oxidation Layer, *Nat. Commun.*, 2024, **15**(1), 783, DOI: 10.1038/s41467-024-44894-z.

14 H. Wu, H. Xu, Y. Shi, T. Yuan, T. Meng, Y. Zhang, W. Xie, X. Li, Y. Li and L. Fan, Recent Advance in Carbon Dots: From Properties to Applications, *Chin. J. Chem.*, 2021, **39**(5), 1364–1388, DOI: 10.1002/cjoc.202000609.

15 J. Shen, Y. Zhu, C. Chen, X. Yang and C. Li, Facile Preparation and Upconversion Luminescence of Graphene Quantum Dots, *Chem. Commun.*, 2011, **47**(9), 2580–2582, DOI: 10.1039/C0CC04812G.

16 S. C. Ray, A. Saha, N. R. Jana and R. Sarkar, Fluorescent Carbon Nanoparticles: Synthesis, Characterization, and Bioimaging Application, *J. Phys. Chem. C*, 2009, **113**(43), 18546–18551, DOI: 10.1021/jp905912n.

17 H. Yang, Y. Liu, Z. Guo, B. Lei, J. Zhuang, X. Zhang, Z. Liu and C. Hu, Hydrophobic Carbon Dots with Blue Dispersed Emission and Red Aggregation-Induced Emission, *Nat. Commun.*, 2019, **10**(1), 1789, DOI: 10.1038/s41467-019-09830-6.

18 Z. Zhang, J. Chen, Y. Duan, W. Liu, D. Li, Z. Yan and K. Yang, Highly Luminescent Nitrogen–doped Carbon Dots for Simultaneous Determination of Chlortetracycline and Sulfasalazine, *Luminescence*, 2018, **33**(2), 318–325, DOI: 10.1002/bio.3416.

19 B. Zhao, H. Ma, M. Zheng, K. Xu, C. Zou, S. Qu and Z. Tan, Narrow–bandwidth Emissive Carbon Dots: A Rising Star in the Fluorescent Material Family, *Carbon Energy*, 2022, **4**(1), 88–114, DOI: 10.1002/cey2.175.

20 T. Meng, T. Yuan, X. Li, Y. Li, L. Fan and S. Yang, Ultrabroad-Band, Red Sufficient, Solid White Emission from Carbon Quantum Dot Aggregation for Single Component Warm White Light Emitting Diodes with a 91 High Color Rendering Index, *Chem. Commun.*, 2019, **55**(46), 6531–6534, DOI: 10.1039/C9CC01794A.

21 W. Hu, L. Li, X. Wang, Y. Zhang, M. Song, L. Shi, X. Hao and S. Lu, Carbonized Polymer Dots: Illuminating Synthesis Pathways, Optical Frontiers, and Photoelectronic Breakthroughs, *Chin. Chem. Lett.*, 2025, **36**(11), 111612, DOI: 10.1016/j.cclet.2025.111612.

22 M. Fernandes Queiroz, K. R. T. Melo, D. A. Sabry, G. L. Sassaki and H. A. O. Rocha, Does the Use of Chitosan Contribute to Oxalate Kidney Stone Formation?, *Mar. Drugs*, 2014, **13**(1), 141–158, DOI: 10.3390/md13010141.

23 S. Shiva Kumar, S. U. B. Ramakrishna, S. V. Krishna, K. Srilatha, B. R. Devi and V. Himabindu, Synthesis of Titanium(IV) Oxide Composite Membrane for Hydrogen Production through Alkaline Water Electrolysis, *S. Afr. J. Chem. Eng.*, 2018, **25**, 54–61, DOI: 10.1016/j.sajce.2017.12.004.

24 M. A. Gabris, B. H. Jume, M. Rezaali, S. Shahabuddin, H. R. Nodeh and R. Saidur, Novel Magnetic Graphene Oxide Functionalized Cyanopropyl Nanocomposite as an Adsorbent for the Removal of Pb(II) Ions from Aqueous Media: Equilibrium and Kinetic Studies, *Environ. Sci. Pollut. Res.*, 2018, **25**(27), 27122–27132, DOI: 10.1007/s11356-018-2749-9.

25 A. F. Shaikh, M. S. Tamboli, R. H. Patil, A. Bhan, J. D. Ambekar and B. B. Kale, Bioinspired Carbon Quantum Dots: An Antibiofilm Agents, *J. Nanosci. Nanotechnol.*, 2019, **19**(4), 2339–2345, DOI: 10.1166/jnn.2019.16537.

26 Y. Wu, H. Zhang, A. Pan, Q. Wang, Y. Zhang, G. Zhou and L. He, White–Light–Emitting Melamine–Formaldehyde Microspheres through Polymer–Mediated Aggregation and Encapsulation of Graphene Quantum Dots, *Adv. Sci.*, 2019, **6**(2), 1801432, DOI: 10.1002/advs.201801432.

27 Y.-P. Sun, B. Zhou, Y. Lin, W. Wang, K. A. S. Fernando, P. Pathak, M. J. Meziani, B. A. Harruff, X. Wang, H. Wang, P. G. Luo, H. Yang, M. E. Kose, B. Chen, L. M. Veca and S.-Y. Xie, Quantum-Sized Carbon Dots for Bright and Colorful Photoluminescence, *J. Am. Chem. Soc.*, 2006, **128**(24), 7756–7757, DOI: 10.1021/ja062677d.

28 J. Xu, Y. Miao, J. Zheng, H. Wang, Y. Yang and X. Liu, Carbon Dot-Based White and Yellow Electroluminescent Light Emitting Diodes with a Record-Breaking Brightness, *Nanoscale*, 2018, **10**(23), 11211–11221, DOI: 10.1039/C8NR01834K.

29 B. Wang, G. I. N. Waterhouse, B. Yang and S. Lu, Advances in Shell and Core Engineering of Carbonized Polymer Dots for Enhanced Applications, *Acc. Chem. Res.*, 2024, **57**(19), 2928–2939, DOI: 10.1021/acs.accounts.4c00516.

30 F. Wang, Y. Chen, C. Liu and D. Ma, White Light-Emitting Devices Based on Carbon Dots' Electroluminescence, *Chem. Commun.*, 2011, **47**(12), 3502, DOI: 10.1039/c0cc05391k.

31 X. Zhang, Y. Zhang, Y. Wang, S. Kalytchuk, S. V. Kershaw, Y. Wang, P. Wang, T. Zhang, Y. Zhao, H. Zhang, T. Cui, Y. Wang, J. Zhao, W. W. Yu and A. L. Rogach, Color-

Switchable Electroluminescence of Carbon Dot Light-Emitting Diodes, *ACS Nano*, 2013, **7**(12), 11234–11241, DOI: 10.1021/nn405017q.

32 F. Yuan, Z. Wang, X. Li, Y. Li, Z. Tan, L. Fan and S. Yang, Bright Multicolor Bandgap Fluorescent Carbon Quantum Dots for Electroluminescent Light–Emitting Diodes, *Adv. Mater.*, 2017, **29**(3), 1604436, DOI: 10.1002/adma.201604436.

33 Y. Ding, F. Zhang, J. Xu, Y. Miao, Y. Yang, X. Liu and B. Xu, Synthesis of Short-Chain Passivated Carbon Quantum Dots as the Light Emitting Layer towards Electroluminescence, *RSC Adv.*, 2017, **7**(46), 28754–28762, DOI: 10.1039/C7RA02421E.

34 F. Yuan, T. Yuan, L. Sui, Z. Wang, Z. Xi, Y. Li, X. Li, L. Fan, Z. Tan, A. Chen, M. Jin and S. Yang, Engineering Triangular Carbon Quantum Dots with Unprecedented Narrow Bandwidth Emission for Multicolored LEDs, *Nat. Commun.*, 2018, **9**(1), 2249, DOI: 10.1038/s41467-018-04635-5.

35 F. Yuan, Y.-K. Wang, G. Sharma, Y. Dong, X. Zheng, P. Li, A. Johnston, G. Bappi, J. Z. Fan, H. Kung, B. Chen, M. I. Saidaminov, K. Singh, O. Voznyy, O. M. Bakr, Z.-H. Lu and E. H. Sargent, Bright High-Colour-Purity Deep-Blue Carbon Dot Light-Emitting Diodes via Efficient Edge Amination, *Nat. Photonics*, 2020, **14**(3), 171–176, DOI: 10.1038/s41566-019-0557-5.

36 T. Zhang, X. Wang, Z. Wu, T. Yang, H. Zhao, J. Wang, H. Huang, Y. Liu and Z. Kang, Highly Stable and Bright Blue Light-Emitting Diodes Based on Carbon Dots with a Chemically Inert Surface, *Nanoscale Adv.*, 2021, **3**(24), 6949–6955, DOI: 10.1039/D1NA00576F.

37 X. Wang, Y. Ma, Q. Wu, Z. Wang, Y. Tao, Y. Zhao, B. Wang, J. Cao, H. Wang, X. Gu, H. Huang, S. Li, X. Wang, F. Hu, M. Shao, L. Liao, T. Sham, Y. Liu and Z. Kang, Ultra–Bright and Stable Pure Blue Light–Emitting Diode from O, N Co–Doped Carbon Dots, *Laser Photonics Rev.*, 2021, **15**(3), 2000412, DOI: 10.1002/lpor.202000412.

38 P. Huang, M.-Z. Li, C.-F. Wen, H.-Y. Zhou, J.-X. Jian and Q.-X. Tong, Nitrogen-Doped Carbon Dots for Efficient Deep-Blue Light-Emitting Diodes with CIE Closely Approaching the HDTV Standard Color Rec.BT.709, *Chem. Commun.*, 2023, **59**(58), 8933–8936, DOI: 10.1039/D3CC02105J.

39 B. Wang, H. Wang, Y. Hu, G. I. N. Waterhouse and S. Lu, Carbon Dot Based Multicolor Electroluminescent LEDs with Nearly 100% Exciton Utilization Efficiency, *Nano Lett.*, 2023, **23**(18), 8794–8800, DOI: 10.1021/acs.nanolett.3c02271.

40 I. Siddiqui, S. Kumar, Y.-F. Tsai, P. Gautam, Shahnawaz, K. Kesavan, J.-T. Lin, L. Khai, K.-H. Chou, A. Choudhury, S. Grigalevicius and J.-H. Jou, Status and Challenges of Blue OLEDs: A Review, *Nanomaterials*, 2023, **13**(18), 2521, DOI: 10.3390/nano13182521.

41 H. Je, S. Cho, N. Y. Kwon, D. W. Lee, M. J. Cho and D. H. Choi, Customized Orthogonal Solvent System with Various Hole-Transporting Polymers for Highly Reproducible Solution-Processable Organic Light-Emitting Diodes, *ACS Appl. Mater. Interfaces*, 2022, **14**(31), 35969–35977, DOI: 10.1021/acsami.2c07659.

42 J. Sun, W. Xu, Y. Liu, B. Sun, J. Xiong, Y. Lian, Y. Lou and L. Feng, Precursor Engineering towards Orange- and Red-Emissive Carbon Dots for LEDs with Tunable Emission Colors, *Nanoscale*, 2025, **17**(3), 1449–1457, DOI: 10.1039/D4NR03184A.

43 F. Mansoori Mosleh, Y. Mortazavi, N. Hosseinpour and A. A. Khodadadi, Asphaltene Adsorption onto Carbonaceous Nanostructures, *Energy Fuels*, 2020, **34**(1), 211–224, DOI: 10.1021/acs.energyfuels.9b03466.

44 W. Gul and H. Alrobei, Effect of Graphene Oxide Nanoparticles on the Physical and Mechanical Properties of Medium Density Fiberboard, *Polymers*, 2021, **13**(11), 1818, DOI: 10.3390/polym13111818.

45 M. Kumari, B. Roul, S. B. Krupanidhi and K. K. Nanda, Heterostructuring Approach to Enhance Figures-of-Merit of Ga2O3 for Deep UV Photodetection, *Phys. B*, 2025, **711**, 417267, DOI: 10.1016/j.physb.2025.417267.

46 H.-K. Jeong, Y. P. Lee, R. J. W. E. Lahaye, M.-H. Park, K. H. An, I. J. Kim, C.-W. Yang, C. Y. Park, R. S. Ruoff and Y. H. Lee, Evidence of Graphitic AB Stacking Order of Graphite Oxides, *J. Am. Chem. Soc.*, 2008, **130**(4), 1362–1366, DOI: 10.1021/ja076473o.

47 H. Jia, Z. Wang, T. Yuan, F. Yuan, X. Li, Y. Li, Z. Tan, L. Fan and S. Yang, Electroluminescent Warm White Light–Emitting Diodes Based on Passivation Enabled Bright Red Bandgap Emission Carbon Quantum Dots, *Adv. Sci.*, 2019, **6**(13), 1900397, DOI: 10.1002/advs.201900397.

48 Z. Wang, N. Jiang, M. Liu, R. Zhang, F. Huang and D. Chen, Bright Electroluminescent White–Light–Emitting Diodes Based on Carbon Dots with Tunable Correlated Color Temperature Enabled by Aggregation, *Small*, 2021, **17**(52), 2104551, DOI: 10.1002/smll.202104551.

49 X. Zhang, Y. Liu, C.-H. Kuan, L. Tang, T. D. Krueger, S. Yeasmin, A. Ullah, C. Fang and L.-J. Cheng, Highly Fluorescent Nitrogen-Doped Carbon Dots with Large Stokes Shifts, *J. Mater. Chem. C*, 2023, **11**(34), 11476–11485, DOI: 10.1039/D3TC02209A.

50 Q. Lou, Q. Ni, C. Niu, J. Wei, Z. Zhang, W. Shen, C. Shen, C. Qin, G. Zheng, K. Liu, J. Zang, L. Dong and C. Shan, Carbon Nanodots with Nearly Unity Fluorescent Efficiency Realized via Localized Excitons, *Adv. Sci.*, 2022, **9**(30), 2203622, DOI: 10.1002/advs.202203622.

51 M. Fu, F. Ehrat, Y. Wang, K. Z. Milowska, C. Reckmeier, A. L. Rogach, J. K. Stolarczyk, A. S. Urban and J. Feldmann, Carbon Dots: A Unique Fluorescent Cocktail of Polycyclic Aromatic Hydrocarbons, *Nano Lett.*, 2015, **15**(9), 6030–6035, DOI: 10.1021/acs.nanolett.5b02215.

52 S. I. Chaudhury, S. Chand, S. Bhuin, S. H. Nandish, N. Yadav and P. Rajamalli, Step-by-Step Guide for Harnessing Organic Light Emitting Diodes by Solution Processed Device Fabrication of a TADF Emitter, *J. Visualized Exp.*, 2025, **225**, e68434, DOI: 10.3791/68434.

53 J. Li, B. Wang, H. Zhang and J. Yu, Carbon Dots–in–Matrix Boosting Intriguing Luminescence Properties and

Applications, *Small*, 2019, **15**(32), 1805504, DOI: 10.1002/smll.201805504.

54 Z.-J. Gao, T.-H. Yeh, J.-J. Xu, C.-C. Lee, A. Chowdhury, B.-C. Wang, S.-W. Liu and C.-H. Chen, Carbazole/Benzimidazole-Based Bipolar Molecules as the Hosts for Phosphorescent and Thermally Activated Delayed Fluorescence Emitters for Efficient OLEDs, *ACS Omega*, 2020, **5**(18), 10553–10561, DOI: 10.1021/acsomega.0c00967.

55 H. Li, Z. Zhang, J. Ding, Y. Xu, G. Chen, J. Liu, L. Zhao, N. Huang, Z. He, Y. Li and L. Ding, Diamond-like Carbon Structure-Doped Carbon Dots: A New Class of Self-Quenching-Resistant Solid-State Fluorescence Materials toward Light-Emitting Diode, *Carbon*, 2019, **149**, 342–349, DOI: 10.1016/j.carbon.2019.04.074.

56 B. Zhi, X. Yao, M. Wu, A. Mensch, Y. Cui, J. Deng, J. J. Duchimaza-Heredia, K. J. Trerayapiwat, T. Niehaus, Y. Nishimoto, B. P. Frank, Y. Zhang, R. E. Lewis, E. A. Kappel, R. J. Hamers, H. D. Fairbrother, G. Orr, C. J. Murphy, Q. Cui and C. L. Haynes, Multicolor Polymeric Carbon Dots: Synthesis, Separation and Polyamide-Supported Molecular Fluorescence, *Chem. Sci.*, 2021, **12**(7), 2441–2455, DOI: 10.1039/d0sc05743f.

57 Y. Zhang, R. Yuan, M. He, G. Hu, J. Jiang, T. Xu, L. Zhou, W. Chen, W. Xiang and X. Liang, Multicolour Nitrogen-Doped Carbon Dots: Tunable Photoluminescence and Sandwich Fluorescent Glass-Based Light-Emitting Diodes, *Nanoscale*, 2017, **9**(45), 17849–17858, DOI: 10.1039/c7nr05363k.

58 B. Wang, J. Yu, S. Ding, H. Wang, Y. Hu and S. Lu, Solution-Processed Near Unit Carbon Dots-Based Deep-Blue Electroluminescent Light-Emitting Diodes with External Quantum Efficiency over 10%, *Nano Lett.*, 2025, **25**(7), 2996–3001, DOI: 10.1021/acs.nanolett.4c06638.